Creeping granular motion under variable gravity levels

Tim Arndt,[1] Antje Brucks,[1] Julio M. Ottino,[2,3] and Richard M. Lueptow[3]
[1]*Zentrum für angewandte Raumfahrttechnologie und Mikrogravitation (ZARM), Universität Bremen, Am Fallturm, 28359 Bremen, Germany*
[2]*Department of Chemical and Biological Engineering, Northwestern University, Evanston, Illinois 60208, USA*
[3]*Department of Mechanical Engineering, Northwestern University, Evanston, Illinois 60208, USA*
(Received 30 June 2006; published 20 September 2006)

In a rotating tumbler that is more than one-half filled with a granular material, a core of material forms that should ideally rotate with the tumbler. However, the core rotates slightly faster than the tumbler (precession) and decreases in size (erosion). The precession and erosion of the core provide a measure of the creeping granular motion that occurs beneath a continuously flowing flat surface layer. Since the effect of gravity on the subsurface flow has not been explored, experiments were performed in a 63% to 83% full granular tumbler mounted in a large centrifuge that can provide very high g-levels. Two colors of 0.5 mm glass beads were filled side by side to mark a vertical line in the 45 mm radius quasi-two-dimensional tumbler. The rotation of the core with respect to the tumbler (precession) and the decrease in the size of the core (erosion) were monitored over 250 tumbler revolutions at accelerations between $1g$ and $12g$. The flowing layer thickness is essentially independent of the g-level for identical Froude numbers, and the shear rate in the flowing layer increases with increasing g-level. The degree of core precession increases with the g-level, while the core erosion is essentially independent of the g-level. Based on a theory for core precession and erosion, the increased precession is likely a consequence of the higher shear rate. Core erosion, on the other hand, is related to the creep region decay constant, which is connected with slow diffusion in the bed and unaffected by gravity.

DOI: 10.1103/PhysRevE.74.031307 PACS number(s): 45.70.Mg, 83.80.Fg

I. INTRODUCTION

The region below a gravity-driven surface flow of granular material once thought to be a "fixed bed" has recently been shown to undergo slow relative displacement of particles [1,2]. Since granular shear flows occur in many geologic and industrial situations including snow and earth avalanches, chutes, hoppers, and mixers, this creeping motion may be of significance, particularly because it may alter the stability, density, and mechanical response of the bulk material. This may be critical in cases where the stability on geological time scales is important.

While gravity drives most granular shear flows in geologic and industrial applications, the effect of changing the gravitational acceleration is largely unexplored for the underlying material below the flowing layer. This may be of particular importance in the understanding of the geology of planets. For instance, avalanches are thought to occur on Mars, Venus, and other planetary bodies [3–10]. In addition, human exploration of the Moon and Mars in the next decades may require excavation or incorporate *in situ* resource utilization. For example, it may be possible to process soil to extract water from below the surface of Mars. Furthermore, exploration of the Mars or Moon will result in the explorers encountering granular material that covers most of the surface. A recent example is the Mars land exploration vehicle getting stuck in loose granular material [11]. Thus, an understanding of the impact of gravity on granular flow is of importance to provide a better understanding of the geology of planetary bodies and to clarify the environments that may be encountered during planetary exploration.

The current understanding of the fundamental physics of gravity-driven granular flows is based almost exclusively on data that was obtained under Earth's gravity. Only a couple of experiments have provided conditions different than $1g$, where g is the gravitational acceleration on Earth. Klein and White examined the flow in a tumbler at gravity levels from $0.02g$ to $1.8g$ on board a parabolic flight aircraft [12]. They found that the dynamic angle of repose of the flowing layer decreases as the g-level increases. More recently, Brucks *et al.* have investigated the validity of the commonly used dimensionless parameter for granular flow in a rotating tumbler, the Froude number, at high gravitational levels [13]. The Froude number, $\mathrm{Fr}=\omega^2 R/g_{\mathrm{eff}}$, where ω is the rotational speed, R is the radius of the tumbler, and g_{eff} is the effective gravitational acceleration, represents the ratio of centrifugal to gravitational forces and is frequently used to characterize the nature of the flow in the canonical case of granular flow in a tumbler [14]. Brucks *et al.* confirmed that the dynamic angle of repose decreases as the g-level increases from $1g$ to $25g$. More importantly, they showed that the angle of repose, flow regime, and shape of the surface of the flowing layer depend only on the Froude number, not directly on g_{eff}, proving that the Froude number properly characterizes the nature of the flowing shear layer when g_{eff} is varied.

In this paper, we investigate the dependence of the subsurface flow on the gravitational level using tumblers that are more than half-filled with granular material. As the tumbler rotates, particles are brought continuously to the surface, avalanche down the slope, and are deposited again in the fixed bed. The surface flow occurs in a lenslike region of maximum depth δ, which is typically 5–12 particles deep [15–19]. Particles in a tumbler filled one-half full or less with identical particles except for color will completely mix within a few tumbler revolutions, because all of the particles pass through the flowing layer at least two times per revolution. The situation is quite different for tumblers that are

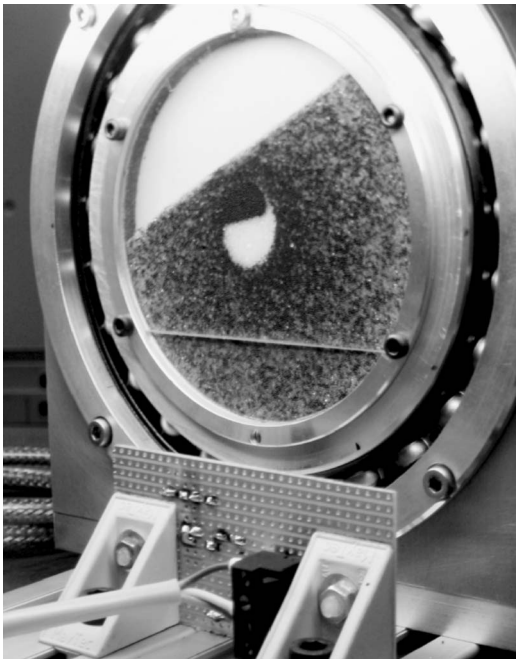

FIG. 1. Image of the tumbler with a core of unmixed particles.

more than one-half full. In this case, an "invariant" circular core region that does not pass through the flowing layer appears at the center of the tumbler, as shown in Fig. 1. Because the material in the core region, which is one-half black and one-half white, does not pass through the flowing layer, the conventional description of tumbler flow assumes that the core is in solid body rotation with the tumbler. However, after many revolutions it is clear that the core rotates with respect to the tumbler (precession) and decreases in size (erosion) [20,21]. Similar patterns have been shown to occur for granular material in a split-bottomed shear cell [22], although the nature of the core motion is quite different in that it is driven by shear of the wall rather than a flowing layer, as is the case here. Recently, we have shown how the core dynamics in a rotating tumbler are driven by the creeping motion beneath the flowing layer. In fact, based on a simple model matching the velocity and shear rate at the boundary between the shear flow and the creeping flow, it can be shown that core precession depends linearly on the number of tumbler revolutions, while the core erosion varies logarithmically with the number of tumbler revolutions [2]. Experimental observations at $1g$ confirm the validity of the model.

Here, we explore the dependence of the subsurface creeping flow on the gravitational level by measuring the core precession and erosion in a rotating tumbler operating under high-g conditions. In addition, we are able to gain insight into the dependence of the flowing layer thickness on g_{eff} and the Froude number. Finally, we examine the impact of the variation in g_{eff} on the parameters of our recent model for core precession and erosion [2] to provide a better understanding of subsurface creeping flow.

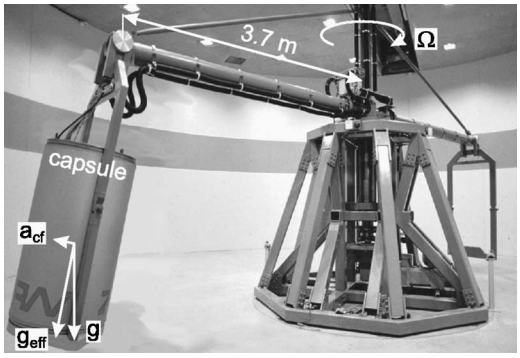

FIG. 2. The centrifuge at ZARM, University of Bremen.

II. EXPERIMENTAL METHODS

Experiments were performed in a 9 cm diameter, quasi-two-dimensional tumbler mounted in the capsule of a large centrifuge. The centrifuge consists of two opposing horizontal arms of length 3.7 m mounted on a vertical shaft that was rotated at speeds up to $\Omega=43.8$ rpm, as shown in Fig. 2. At the end of one arm is a 0.65 m diameter by 1.8 m long capsule containing the experimental apparatus. The capsule pivots at the end of the arm so that the effective gravitational acceleration, $\mathbf{g}_{\mathrm{eff}}$, which is the vector sum of Earth's gravity vector, $\mathbf{g}$, and the centrifugal acceleration vector, $\mathbf{a}_{cf}$, is directed along the capsule's axis. A counter-weight is mounted on the opposite arm of the centrifuge. When the capsule is fully extended so its axis is horizontal, as occurs at high rotational speeds, the radius to the bottom of the capsule is 6.33 m.

The experimental apparatus, including tumbler, camera, light, and computer control system, was mounted inside the capsule. A slip ring permitted electrical power supply and data connection between the capsule and the laboratory. The $R=4.5$ cm radius tumbler was designed so that the body of the tumbler was within a very large ball bearing in order to withstand the high g-levels, as shown in Fig. 1. The tumbler, which was made of aluminum with a clear glass side wall to permit optical access, has a thickness of $t=0.5$ cm $\approx 9.4d$, where d is the particle diameter. This cell thickness is sufficient to prevent particles from jamming, but thin enough to suppress axial effects. The circumferential wall of the tumbler was covered with 60-grit sandpaper to minimize slippage of the granular bed with respect to the tumbler. The tumbler was driven at a constant angular velocity by a computer-controlled dc motor with planetary gear reduction and feedback control via an encoder mounted on the motor shaft. The clear sidewall was split horizontally one-quarter of the tumbler diameter above the horizontal axis of the tumbler to permit filling the tumbler with particles.

A digital camera was mounted concentric with the axis of the tumbler to acquire images of the granular media. A photosensor was used to determine the tumbler rotational position and trigger the camera. After an experiment, images stored on the camera's flash memory card were downloaded onto a computer for analysis. An accelerometer mounted at the same level as the tumbler axis measured the effective g-level.

Two colors of similar glass beads were used. It is difficult to find beads that provide adequate optical contrast that are otherwise identical. The 0.53 mm±0.05 mm black beads had a density of 2.9 g/cm^3, while the 0.55 mm±0.03 mm white beads had a density of 2.5 g/cm^3. Because of concern that the slight density and size difference could result in segregation, tests were performed using a 50-50 mixture of the beads in a half-full tumbler for up to 1000 tumbler revolutions at $1g$ and $12g$. Only a slight tendency toward segregation was barely perceptible. This is not surprising given that the mass of the particles differ by less than 4% and that the downward percolation of the smaller black particles should be offset to some extent by upward buoyancy of the white particles [23]. Since the effects of segregation are evident only after a very large number of revolutions in a half-full tumbler and the experiments described here involve tumblers that are more than half-full, so the entire body of material outside of the core is remixed in less than one revolution, we assume that size and density segregation play little role in the measurements described here.

The experiments were initiated with the left half of the tumbler partially filled with black beads and the right half with white beads to the desired fill levels. The fill fraction, f, defined as the ratio of the volume occupied by the particles (including the interstitial space) to the total tumbler volume, was set at $f=0.631$, 0.705, and 0.829, the first two values of which are identical to the previous study at $1g$ [2]. The rotational speed was set at $\omega=1.40$ rpm to 4.87 rpm for nominal g-levels from $1g$ to $12g$ to maintain the Froude number, $\mathrm{Fr}=\omega^2 R/g_{\mathrm{eff}}$, between 9.78×10^{-5} and 9.93×10^{-5}, consistent with a Froude number of 9.86×10^{-5} in the previous study [2]. The continuously flowing surface remained flat, known as the rolling regime of flow [14,24], at this Froude number.

Each experiment began by bringing the centrifuge to the desired speed to set the g-level with the tumbler not rotating. Based on the location of the surface of the bed, it was evident that changes in the packing fraction in the bed of particles due to the increased g-level were negligible. Once a constant g-level was maintained, the tumbler rotation was started. Images were acquired every five rotations beginning with the initial condition. Since previous results indicate that core precession and erosion are established within 10 rotations and continue for at least 1000 rotations [2], experiments were performed for only the first 250 rotations of the tumbler.

The core is defined as the circular domain of unmixed particles at the center of the tumbler. Its radius was measured on the tumbler image by visually fitting a circle concentric with the tumbler to the location of the transition between the core and the fixed bed of particles. The precession of the core was measured as the angle between vertical and the boundary between white and black particles. Typically, the center 70% of the boundary was used to determine the precession angle, because the boundary is curved near the edge of the core.

One concern with performing experiments in a centrifuge is the impact of the Coriolis acceleration, $2\boldsymbol{\Omega}\times\mathbf{V}$, where $\mathbf{V}$ is the velocity of particles in the rotating frame. (For these experiments, the axis of the tumbler was in the plane defined by the centrifuge arm and centrifuge axis of rotation.) The surface velocity of flowing layer can be estimated from mass conservation in the tumbler and the components of velocity can be determined based on the angle of repose and the angle of the capsule with respect to the centrifuge shaft. Using these values, the ratio of the Coriolis acceleration to the g-level was estimated to be less than 0.02, which is assumed to be inconsequential.

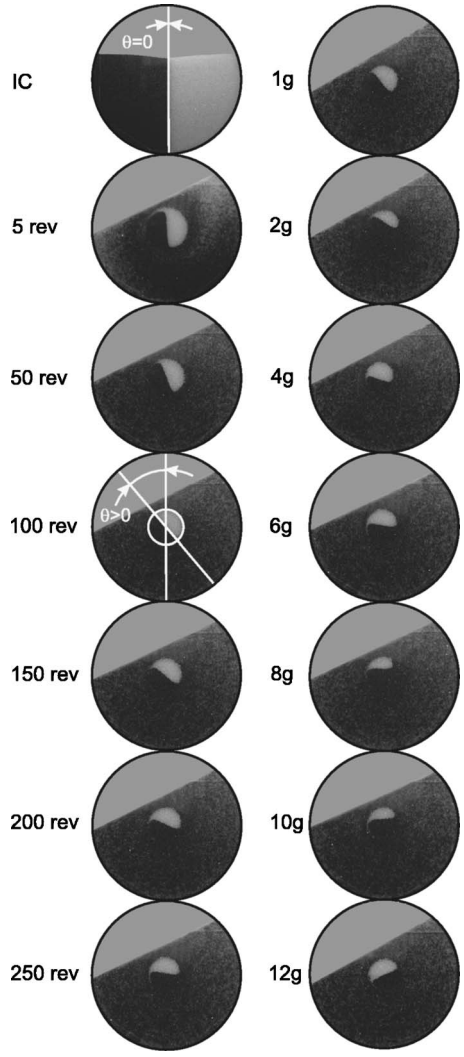

FIG. 3. Images of the tumbler showing core precession θ and erosion. The core is the half-black and half-white circular region at the center of the tumbler. The tumbler rotates counter-clockwise. The left-hand column of images shows the evolution of the core from the initial condition (IC) to 250 revolutions for $f=0.705$ at $6g$. The right-hand column of images shows the dependence of the core at $N=250$ revolutions on the nominal gravitational level for $f=0.705$.

III. RESULTS

The typical evolution of the circular core is shown on the left-hand side of Fig. 3 for a fill fraction of $f=0.705$ at $6g$. The angular position of the core with respect to vertical increases in the direction of tumbler rotation (precession), and the size of the core decreases (erosion) as the number of

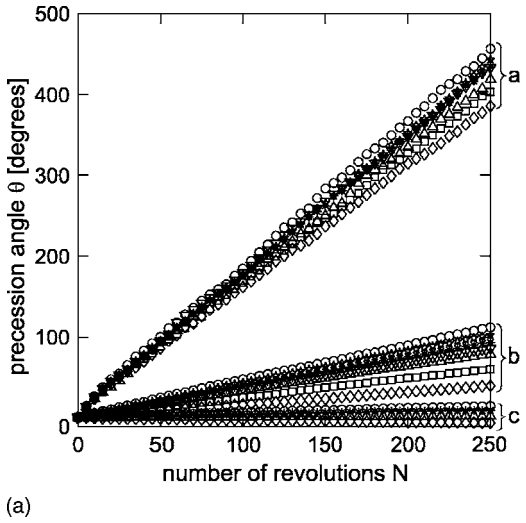

FIG. 4. Dependence of precession angle θ on the number of revolutions N for $f=0.631$ (a), $f=0.705$ (b), and $f=0.829$ (c). Symbols: ◇, 1.00g; □, 2.03g; △, 4.05g; ∇, 6.09g; *, 8.08g; ⋆, 10.08g; ◦, 12.07g.

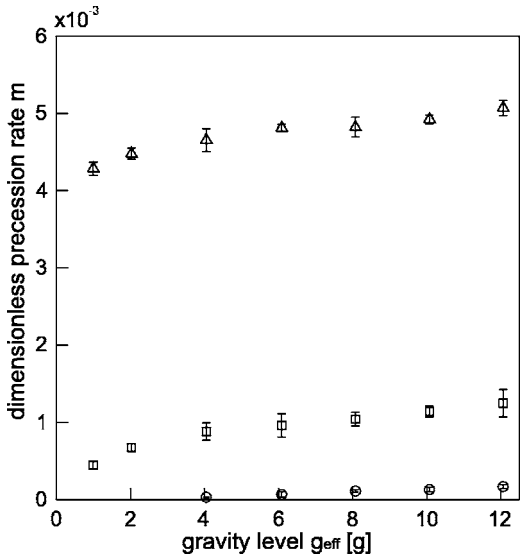

FIG. 5. Dependence of the dimensionless precession rate m on the gravitational level. Symbols: △, $f=0.631$; □, $f=0.705$; ◦, $f=0.829$. Error bars are ± one standard deviation.

rotations of the tumbler increases, consistent with measurements at 1g [2]. What is perhaps more interesting is the dependence of the final state after 250 rotations on the g-level, as shown on the right-hand side of Fig. 3. Clearly, precession increases with g-level. The size of the core, however, does not appear to depend on the g-level.

Consider first the core precession. The dependence of the precession angle, θ, on the number of revolutions, N, is shown in Fig. 4 for the three fill fractions. The results are averaged over three experiments for $f=0.631$ and $f=0.829$ and over five experiments for $f=0.705$. The precession angle is much greater for small fill ratios than for larger fill ratios and increases linearly with the number of revolutions, consistent with previous results at 1g [2]. Increasing the g-level results in a larger precession angle, regardless of fill fraction. At a fill fraction of $f=0.829$, the precession angle is positive, though quite small for high g-levels. The precession angle is slightly negative, however, for 1g and 2g, most likely due to slippage of the bed of particles with respect to the tumbler. Similarly results were observed for 1g at high fill levels [2].

The dimensionless precession rate, m, shown in Fig. 5 is defined as the change in θ (in radians) per radian of tumbler rotation, which corresponds to the slope of the data in Fig. 4. Clearly the precession rate increases slightly with g-level. Assuming an approximately linear decrease in velocity with depth in the flowing layer [17] and an exponential decay of the velocity in the creeping flow below the flowing layer [1,15,25], it can be shown that [2]

$$m(g_{\text{eff}}) = \frac{\dot{\gamma}(g_{\text{eff}})}{2\omega} e^{[\delta(g_{\text{eff}})-b]/y_0(g_{\text{eff}})}, \tag{1}$$

where δ is the flowing layer depth, $\dot{\gamma}$ is the shear rate in the flowing layer, b is the perpendicular distance from the surface of the flowing layer to the center of the tumbler, and y_0 is a decay constant for the creeping flow velocity profile. Only certain variables in this expression, δ, $\dot{\gamma}$, and y_0, could potentially be functions of the g-level. Since the granular bed does not compress as g_{eff} is increased, b does not depend on g_{eff}. Closer examination of the data permits the determination of which of these variables carry the dependence on g_{eff}.

The flowing layer depth can be readily determined based on the images of the tumbler after the core has clearly formed (in this case after five revolutions of tumbler), as is evident from Figs. 1 and 3. The flowing layer depth is simply $\delta=b-r_0$, where r_0 is the initial radius of the nonflowing core. The flowing layer thickness determined in this way is shown in Fig. 6. The flowing layer depth increases with fill level, but more important to this discussion is that the flowing layer depth is essentially independent of g-level (within the scatter

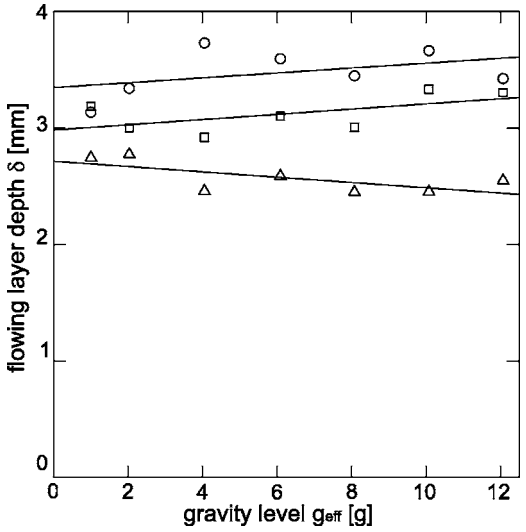

FIG. 6. Dependence of the flowing layer thickness δ on the gravitational level. Symbols: △, $f=0.631$; □, $f=0.705$; ◦, $f=0.829$. Lines are linear fits to the data. The average standard deviation is ±0.20 mm for $f=0.631$, ±0.40 mm for $f=0.705$, and ±0.77 mm for $f=0.829$.

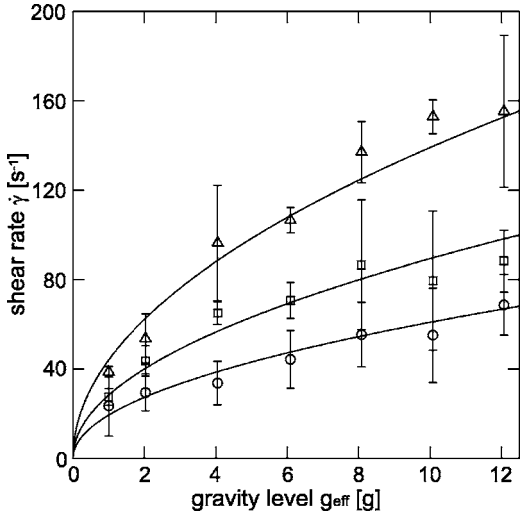

FIG. 7. Dependence of the flowing layer shear rate on the gravitational level. Symbols: △, $f=0.631$; □, $f=0.705$; ◦, $f=0.829$. The curves are based on Eq. (3). Error bars, which represent ± one standard deviation, are fairly large in some cases due to the difficulty in accurately measuring the flowing layer thickness δ.

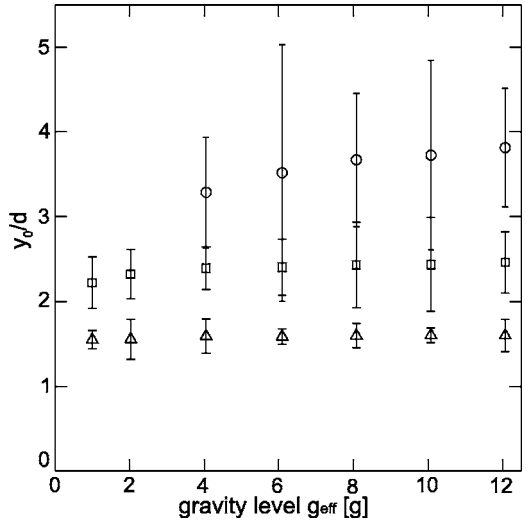

FIG. 8. Dependence of the creeping flow decay constant y_0 on the gravitational level based on core precession. Symbols: △, $f=0.631$; □, $f=0.705$; ◦, $f=0.829$. Error bars, which represent ± one standard deviation, are fairly large for $f=0.829$ due to the difficulty in accurately measuring the flowing layer thickness δ and estimating the shear rate $\dot{\gamma}$.

of the data). This is an important result, given that it would be reasonable to expect that the flowing layer might dilate less at high g-levels. This is not the case, suggesting that the dilation of the flowing layer is only enough to permit the motion of particles down the slope.

Once the flowing layer thickness is known, the shear rate in the flowing layer can be estimated as u_{surf}/δ, where u_{surf} is the velocity at the top surface. The number density of particles in the flowing layer is assumed to be similar to that in the fixed bed, as is typically used as a first approximation in a half-filled tumbler at $1g$ [15]. Then the volume flow rate in the flowing layer must match that in the fixed bed by mass conservation. Assuming a linear velocity profile in the flowing layer [15], the volume flow rate in the flowing layer is $\delta u_{surf}/2$. Since the average velocity in the fixed bed outside of the core is $\omega(R+r_0)/2$, the volume flow rate in the fixed bed is $(R-r_0)[\omega(R+r_0)/2]$. Setting these flow rates equal and using the approximation for the shear rate, it is straightforward to show that

$$\dot{\gamma} \approx \frac{\omega(R^2 - r_0^2)}{\delta^2}. \tag{2}$$

Using the values for δ from Fig. 6 and the measured initial core radius, r_0, the shear rate can be determined for each g-level and fill level. As shown in Fig. 7, the shear rate is strongly dependent on the g-level. The reason for this is quite simple. In these experiments, the tumbler's rotational speed is increased as the g-level is increased to keep the Froude number constant. As the rotational speed of the tumbler increases, granular material must flow at a higher rate to account for the increased rate at which particles are brought into the flowing layer from the fixed bed. Since the flowing layer thickness does not change, as shown in Fig. 6, the velocity of the particles increases to provide the higher flow rate. The higher velocity of particles in a flowing layer of unchanged thickness results in a higher shear rate. In fact, expressing the tumbler rotational speed in terms of the Froude number and substituting into Eq. (2) results in

$$\dot{\gamma} = \frac{R^2 - r_0^2}{\delta^2}\sqrt{\frac{\mathrm{Fr} g_{eff}}{R}}. \tag{3}$$

Thus, the shear rate should depend on the square root of the gravitational level for constant Froude number. Equation (3) is plotted for each fill level in Fig. 7 using the fixed values for R and Fr, the measured value for r_0, and the average value from Fig. 6 for δ. The data for each fill level match this dependence on g_{eff} reasonably well. The dependence of the shear rate but not the flowing layer thickness on the g-level is not surprising based on dimensional arguments alone. Since the only variables in the problem that include time are the shear rate and the g-level, it is expected that the shear rate should depend on the g-level.

Finally, we consider the dependence of the creep region decay constant, y_0, on g_{eff}. This can be readily accomplished by rearranging Eq. (1) to solve for y_0.

$$y_0 = \frac{\delta - b}{\ln(2m\omega/\dot{\gamma})}. \tag{4}$$

Since b and ω are set during the experiment, and δ, m, and $\dot{\gamma}$ are measured, y_0 can be calculated for each fill level and g-level. The results are shown in Fig. 8, where y_0 is nondimensionalized by the particle diameter. There appears to be a slight dependence of y_0 on the g-level, particularly at the highest fill level. This is not surprising given that y_0 represents the distance over which the velocity in the creep flow region is correlated. As the g-level increases, it is likely that the interparticle contact forces are stronger leading to a longer distance over which particle motions are correlated as

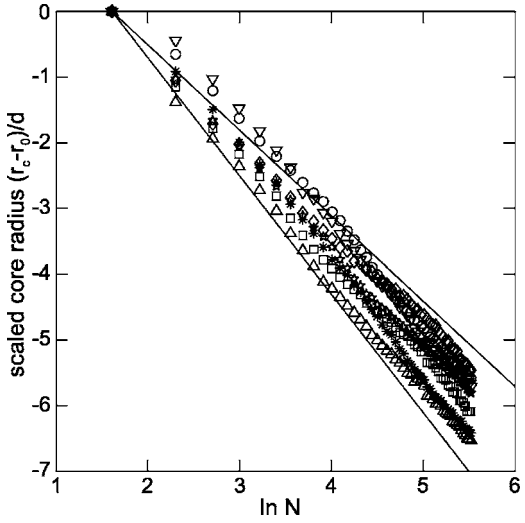

FIG. 9. Dependence of core radius r_c on the number of revolutions N for $f=0.705$. Symbols: ◇, $1.00g$; □, $2.03g$; △, $4.05g$; ∇, $6.09g$; *, $8.08g$; ⋆, $10.08g$; ∘, $12.07g$.

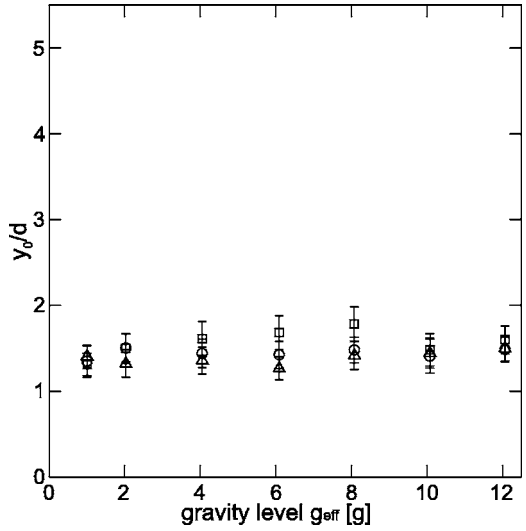

FIG. 10. Dependence of the creeping flow decay constant y_0 on the gravitational level based on core erosion. Symbols: △, $f=0.631$; □, $f=0.705$; ∘, $f=0.829$. Error bars are ± one standard deviation.

particles slowly shift with respect to one another. The values for y_0 at all g-levels and fill levels are similar to previous results giving a range of y_0 from $1.4d$ to $3.4d$ for a variety of flow conditions [1,2,25]. Not only does this similarity in values confirm that the results shown here are reasonable, it confirms the validity of the basis for the model for core precession developed by Socie *et al.* [2].

Now we return to the model for core precession, Eq. (1). The dependence of m on g_{eff} appears to be related to a large extent on the dependence of $\dot{\gamma}$ on g_{eff} and to a much lesser extent of y_0 on g_{eff}. However, previous work at $1g$ [2] resulted in values for m that are substantially smaller than those found in these experiments at $1g$. This difference is likely due to the differences in bead size (0.89 mm versus 0.54 mm here) and tumbler diameter (17.8 cm versus 9 cm here).

Of course, core erosion is the second aspect of core dynamics in a rotating tumbler that is more than half-full. A model for core erosion based on the exponential velocity profile in the creep flow region and a diffusion coefficient related to the particle diameter and the relative velocity difference across a particle indicates that [2]

$$\frac{r_c - r_0}{d} = -\frac{y_0}{d}\ln(N), \tag{5}$$

where r_c is the core diameter at rotation N. Recall that y_0/d is not strongly dependent on g_{eff} (Fig. 8). Also $r_c=b-\delta$ is essentially independent of g_{eff} since δ is not strongly dependent on g (Fig. 6). Thus, it is not surprising that the core size depends on N (as shown on the left-hand side of Fig. 3), but not on g_{eff} (as shown on the right-hand side of Fig. 3).

This result can be further amplified by plotting the normalized change in core size, $(r_c-r_0)/d$, as a logarithmic function of N, as shown in Fig. 9 for $f=0.705$. It is immediately evident that the functional form predicted by Eq. (5) is appropriate regardless of g-level. However, the data for the different g-levels do not follow a logical order in terms of slope, which by Eq. (5) is y_0/d. The $1g$ data has the smallest slope ($y_0/d \approx 1.3$), and the $4g$ data has the largest slope ($y_0/d \approx 1.8$), with the slopes of the other g-levels randomly distributed between these two values. Results are similar in nature for the other two fill levels (not shown), although the range of values for the slope y_0/d are smaller.

Figure 10 shows the dependence of y_0/d as calculated based on the slope of the data in Fig. 9 and corresponding figures for other fill levels. The value for y_0/d is essentially constant with g-level. This further confirms that the core size is essentially independent of g-level. Finally, note that the values for y_0/d shown in Fig. 10 are consistent with the previous value of $y_0/d \approx 1.5$ obtained at $1g$ with a larger tumbler and larger particles [2]. Of course, the values for y_0/d obtained based on the precession data (Fig. 8) and based on the erosion data (Fig. 10) are somewhat different. Although the values for the smallest fill fraction are similar, the values for the largest fill fraction differ by as much as a factor of 2.5. This is not unexpected given that similar results were obtained at $1g$ by Socie *et al.* [2]. Nevertheless, the values are reasonably similar given that the models for core precession are quite different: one is based on matching the velocity profile at the interface between the core and the flowing layer, while the other is based on a local diffusion coefficient. Furthermore, both models rely on the assumptions of relatively simple forms for the velocity profiles and the diffusion coefficient. Thus, the key result with regard to the decay constant, y_0, is that its value is on the order of a few particle diameters. This is reasonable given the nature of the flow in the creep region, where is it expected that the influence of the velocity should be localized to within a few particle diameters. It is also consistent with previous estimates of y_0 between $1.4d$ and $3.4d$ [1,2,25].

IV. CONCLUSIONS

These measurements in which the g-level is varied in addition to the fill level provide insight into the nature of the

subsurface creeping flow beneath a flowing granular layer. The precession rate of the core, m, depends on g-level primarily through the dependence of the shear rate on g_{eff}. Thus, it appears that precession is driven by the shear rate. This is not unreasonable based on a simplistic view of the situation: the flowing layer drags the core along with it causing the core to rotate in the direction of the flow. As the shear in the layer increases, the tendency for the flowing layer to drag the core along with it increases.

Erosion, on the other hand, is nearly independent of the g-level and, hence, independent of the shear rate. This suggests that the erosion is not affected by the details of the flowing layer. In fact, the model for erosion indicates that the erosion should depend only on the decay constant, y_0, for the creep velocity. That the decay constant is independent of the g-level suggests erosion is a local diffusional effect. While an adjacent flowing layer is needed for the erosion, the erosion is not strongly dependent on the nature of the flowing layer. This is further amplified by noting that similar values for y_0/d have been found for chute flows [1,25].

Returning now to one of the motivations for this work, that of granular flow at low gravity levels such as the case on Mars or the Moon, several comments can be made. It appears that the flow in the creep region is largely independent of g_{eff} and the details of the flowing layer above. This has profound consequences for the modeling of subsurface flow soil mechanics: the gravity level probably does not play a role. Of course, the g-level plays a significant role in the surface flow. In fact, one of the key results of this work apart from core dynamics is the dependence of the flowing layer on the g-level. It is evident that for a constant Froude number the flowing layer thickness is independent of g_{eff}, while the shear rate in the flowing layer depends on $\sqrt{g_{\mathrm{eff}}}$.

Although the results described here were obtained for gravitational levels greater than $1g$, the nature of the dependence on g_{eff} suggests that the relationships can be extrapolated to less than $1g$. Thus, the character of a flowing layer on planetary bodies can be predicted to some extent. In particular, it is likely that the flowing layer thickness is a function of particle size alone. In these experiments using 0.5 mm spherical particles, the flowing layer was typically $5d$ to $7d$, regardless of g-level, consistent with experiments at $1g$ where the flowing layer thickness is typically $5d$ to $12d$ [15–17,26]. (Of course, the granular material on the surface of the Moon or Mars has substantially different characteristics than mm-size spherical particles, so the flowing layer thickness could be quite different.) The shear rate in the flowing layer, however, is much higher at high g-levels than at low g-levels. One might then speculate that an avalanche on the surface of Mars would probably have the same depth as one on Earth, but would flow at a substantially slower speed.

Many other questions arise, based on this work. In particular, the details of the flow field, both the velocity profile and the particle number density profile, under different g-levels are unknown. Based on the experiments presented here, the shear rate in the flowing layer will increase with g-level. But it is not clear that the velocity profile will retain a linear form at high (or low) g-levels. Of course, the experiments described here were for the rolling regime of flow, a continuous flow with a flat surface. The effect of g-level on avalanching flow, where the surface flow is intermittent, and cataracting flow, where the surface of the flowing layer is curved, need investigation.

ACKNOWLEDGMENT

The authors thank the University of Bremen for funding this work.

[1] T. S. Komatsu, S. Inagaki, N. Nakagawa, and S. Nasuno, Phys. Rev. Lett. **86**, 1757 (2001).
[2] B. A. Socie, P. Umbanhowar, R. M. Lueptow, N. Jain, and J. M. Ottino, Phys. Rev. E **71**, 031304 (2005).
[3] A. T. Basilevsky and J. W. Heap, Rep. Prog. Phys. **66**, 1699 (2003).
[4] M. F. Gerstell, O. Aharonson, and N. Schorghofer, Icarus **168**, 122 (2004).
[5] K. A. Howard, Science **180**, 1052 (1973).
[6] M. C. Malin, J. Geophys. Res. **97**, 16337 (1992).
[7] A. S. McEwan, Geology **17**, 1111 (1989).
[8] P. M. Schenk and M. H. Bulmer, Science **279**, 1514 (1998).
[9] T. Shinbrot, N.-H. Duong, L. Kwan, and M. M. Alvarez, Proc. Natl. Acad. Sci. U.S.A. **101**, 8542 (2004).
[10] A. H. Treiman, J. Geophys. Res. **108**, 8031 (2003).
[11] G. Webster, http://marsrovers.jpl.nasa.gov/newsroom/pressreleases/20050506a.html(2005).
[12] S. P. Klein and B. R. White, AIAA J. **28**, 1701 (1990).
[13] A. Brucks, T. Arndt, J. M. Ottino, and R. M. Lueptow (unpublished).
[14] J. M. Ottino and D. V. Khakhar, Annu. Rev. Fluid Mech. **32**, 55 (2000).
[15] N. Jain, J. M. Ottino, and R. M. Lueptow, Phys. Fluids **14**, 572 (2002).
[16] D. V. Khakhar, A. V. Orpe, and J. M. Ottino, Adv. Complex Syst. **4**, 407 (2001).
[17] N. Jain, J. M. Ottino, and R. M. Lueptow, J. Fluid Mech. **508**, 23 (2004).
[18] A. V. Orpe and D. V. Khakhar, Phys. Rev. Lett. **93**, 068001 (2004).
[19] K. M. Hill, G. Gioia, and V. V. Tota, Phys. Rev. Lett. **91**, 064302 (2003).
[20] J. J. McCarthy, T. Shinbrot, G. Metcalfe, J. E. Wolf, and J. M. Ottino, AIChE J. **42**, 3351 (1996).
[21] G. Metcalfe, T. Shinbrot, J. J. McCarthy, and J. M. Ottino, Nature (London) **374**, 39 (1995).
[22] D. Fenistein, J.-W. van de Meent, and M. van Hecke, Phys. Rev. Lett. **96**, 118001 (2006).
[23] N. Jain, J. M. Ottino, and R. M. Lueptow, Granular Matter **7**, 69 (2005).
[24] H. Henein, J. K. Brimacombe, and A. P. Watkinson, Metall. Trans. B **14B**, 191 (1983).
[25] D. Bonamy, F. Daviaud, and L. Laurent, Phys. Fluids **14**, 1666 (2001).
[26] A. V. Orpe and D. V. Khakhar, Phys. Rev. E **64**, 031302 (2001).